RSC Advances

PAPER

View Article Online
View Journal | View Issue

Cite this: *RSC Adv.*, 2019, **9**, 14343

A supported manganese complex with amine-bis(phenol) ligand for catalytic benzylic C(sp^3)–H bond oxidation†

Touraj Karimpour,[a] Elham Safaei*[b] and Babak Karimi[a]

Received 25th March 2019
Accepted 25th April 2019

DOI: 10.1039/c9ra02284h

rsc.li/rsc-advances

With regards to the importance of direct and selective activation of C–H bonds in oxidation processes, we develop a supported manganese amine bis(phenol) ligand complex as a novel catalyst with the aim of obtaining valuable products such as carboxylic acids and ketones that have an important role in life, industry and academic laboratories. We further analyzed and characterized the catalyst using the HRTEM, SEM, FTIR, TGA, VSM, XPS, XRD, AAS, and elemental analysis (CHN) techniques. Also, the catalytic evaluation of our system for direct oxidation of benzylic C–H bonds under solvent-free condition demonstrated that the heterogeneous form of our catalyst has high efficiency in comparison with homogeneous ones due to more stability of the supported complex. Furthermore, the structural and morphological stability of our efficient recyclable catalytic system has been investigated and all of the data proved that the complex was firmly anchored to the magnetite nanoparticles.

Introduction

From the environmental and economic points of view, the functionalization of the organic substrates is one of the best strategic approaches for the preparation of broad ranges of new chemicals as a novel and attractive way in organic synthesis.[1] Because of the accessibility of carbon–hydrogen bonds in organic substrates, the activation of these bonds is an attractive and challenging method for selective synthesis of products with different functional groups. It is noteworthy that the methane monooxygenases (MMOs) and cytochrome P-450 are two important classes of enzymes that are applied by nature to attain high selectivity in the oxidation of alkanes at elevated rates.[2] Two identified forms of the MMOs which contain iron or copper ions in their active sites are able to produce methanol from methane.[3] The cytochrome P-450 uses its iron porphyrin core to catalyze the oxidation of hydrocarbons to alcohols through the carbon–hydrogen activation method with high turnover numbers.[4] Several interesting homogenous catalytic systems involving transition-metals (Cu,[5] Fe,[6] Mn,[7] Co,[8] Ni,[9] Pd,[10] Rh,[11] Ru[12] and Ti[13]) have been reported for this important process. These systems have limited applications in comparison with the heterogeneous catalysis, due to product separation and catalyst recycling problems.

In the past decade, immobilization of metal complexes on various supports has been introduced and investigated to overcome the problems pertaining to unsupported complexes. So this catalytic system has the privileges of both homogeneous and heterogeneous catalysts. From a sustainable point of view, the core–shell magnetic nanoparticles (MNPs) are quite favourable supports.[14] These magnetized catalysts can be easily isolated by applying an appropriate magnetic field. This unique characteristic of MNPs eliminates the necessity of procedures such as centrifugation or filtration for the recycling of the catalysts. Despite of several interesting reports[15] for activation of the inert C–H bonds, there are limited publications that address the issue of heterogeneous C–H oxidation catalysis using Earth-abundant iron[16] and manganese catalysts.[17]

Due to the special importance of C–H bond oxidation in the pharmaceutical and chemical industries, and ideal properties of both manganese complexes and magnetic nanoparticles, our main aim is designing a novel, sustainable and selective heterogeneous system for benzylic C–H bond oxidation. Regarding the fact that amine bis(phenol) ligands consist of N and O atoms, and different substituents on the phenol groups, they are able to tune the Lewis acidity of the metal centres which plays a crucial role in the catalytic activity of metal complexes. Consequently, an amine bis(phenol) ligand was applied to design our catalyst. The immobilized amine bis(phenolate) ligand on the magnetite nanoparticles (Fe_3O_4@SiO_2-APTES-H_2L^{GDC}) was prepared according to the previous report in our group.[18] Manganese as an inexpensive, Earth-abundant and non-toxic metal was applied for metalation of these nanoparticles. It is interesting to note that we found the high cooperation between silica-coated Fe_3O_4 nanoparticles and

[a]Department of Chemistry, Institute for Advanced Studies in Basic Sciences (IASBS), P. O. Box 45137-66731, Gava Zang, Zanjan, Iran

[b]Department of Chemistry, College of Sciences, Shiraz University Shiraz, 71454, Iran. E-mail: e.safaei@shirazu.ac.ir

† Electronic supplementary information (ESI) available. See DOI: 10.1039/c9ra02284h

manganese complex for the synthesis of a sustainable catalyst. In our designed system the stabilized manganese complex exhibits excellent efficiency in selective benzylic C–H bond oxidation for a wide range of substrates as well as toluene. Furthermore, five successful recoveries of the catalyst confirmed the stability of the manganese complex attached to the magnetic nanoparticles.

Results and discussion

Synthesis and characterization of Fe_3O_4@SiO_2-APTES-MnL^{GDC}

Using the presented route in Scheme 1, immobilized amine bis(phenol) ligand on the magnetite nanoparticles (Fe_3O_4@SiO_2-APTES-H_2L^{GDC}) was prepared according to the previously report in our group,[18] afterward for metalation of these nanoparticles $MnCl_2 \cdot 4H_2O$ was applied (Scheme 1).

Both chemical nature and structure of our catalyst have been investigated *via* the common methods. The powder X-ray diffraction (XRD) analysis was performed in order to obtain information about the phase purity and crystalline structure of Fe_3O_4@SiO_2, Fe_3O_4@SiO_2-APTES, Fe_3O_4@SiO_2-APTES-H_2LGDC and Fe_3O_4@SiO_2-APTES-MnL^{GDC} (Fig. 1A). Our results are in line with previous reports of Fe_3O_4@SiO_2 nanoparticles XRD pattern.[19] XRD pattern for all nanoparticles show the cubic inverse spinel of Fe_3O_4 nanoparticles and a broad diffraction peak in the $2\theta = 20$–30°, demonstrating the presence of silica shell. Diffraction peaks of [111], [220], [311], [400], [422], [511], and [440] planes found in 18, 30, 35, 43, 54, 57 and 63 degree, respectively.

FT-IR analysis was used to investigate the successful functionalization and modification of particles. As can be seen in Fig. 1B, broad peak at 3423 cm^{-1} is related to the O–H and N–H vibrations and the presence of stretching vibration of Fe–O in all samples was found (at around 544 cm^{-1}). Moreover, symmetric stretching (at about 400 and 800 cm^{-1}, respectively), asymmetric stretching of Si–O–Si (at about 1200 cm^{-1}) and

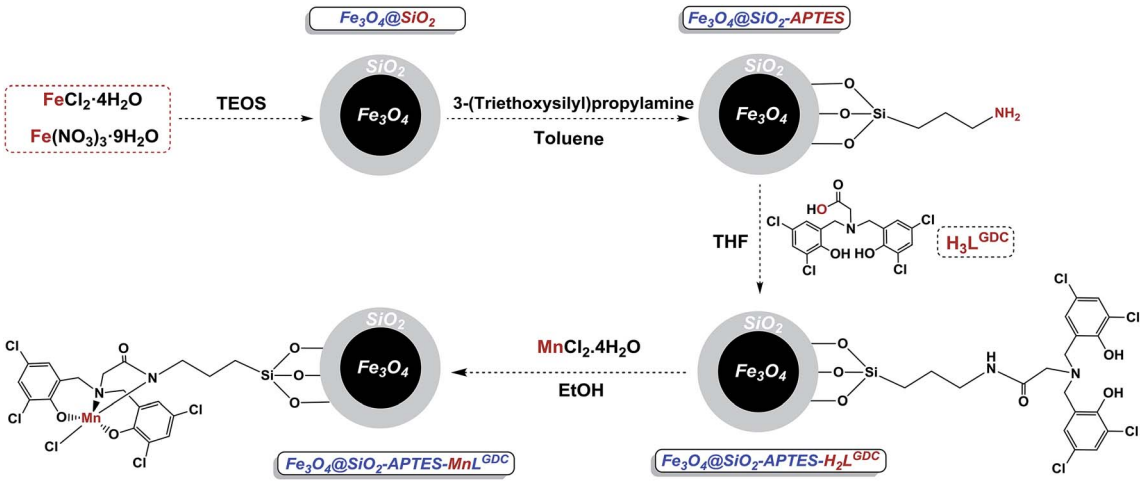

Scheme 1 A schematic illustration of catalyst (Fe_3O_4@SiO_2-APTES-MnL^{GDC}).

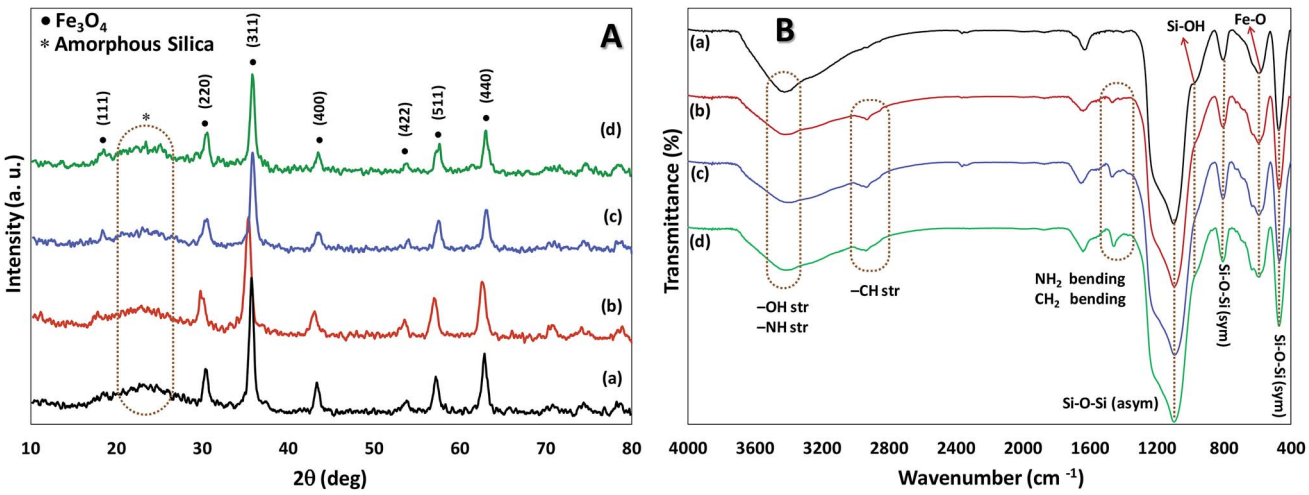

Fig. 1 (A) The XRD pattern, (B) the FTIR spectra of Fe_3O_4@SiO_2 (a), Fe_3O_4@SiO_2-APTES (b), Fe_3O_4@SiO_2-APTES-H_2L^{GDC} (c) and Fe_3O_4@SiO_2-APTES-MnL^{GDC} (d).

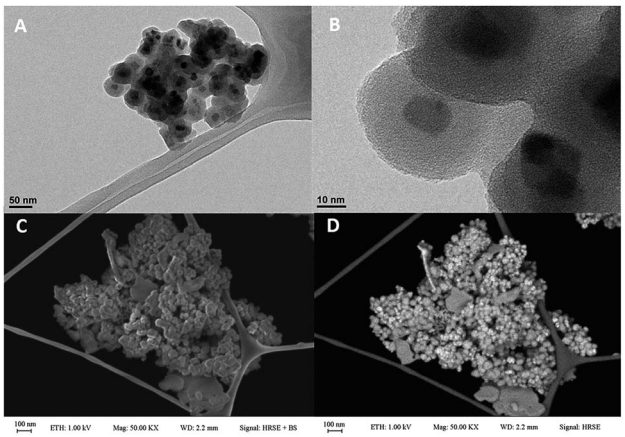

Fig. 2 HRTEM (A and B) and FESEM (C and D) images of Fe_3O_4@SiO_2-APTES-MnL^{GDC}.

stretching vibrations of Si–OH (at around 900 cm^{-1}) are evidence to support the existence of silica shell in all magnetic nanoparticles.[20] Bending peak of $-CH_2$ at 1400 cm^{-1} and stretching vibrations peaks related to $-CH_2$ and N–H groups at about 2840–3000 cm^{-1} and 3400 cm^{-1}, respectively, confirmed stabilization of amino propyl groups on the particles.

The HRTEM and FESEM analyses played a crucial role in the investigation of size, structure, and morphology of nanomagnetic particles. Our results show that nanoparticles are smaller than 45 nm and core size is about 15 nm that surrounded *via* 15 nm uniform grey silica shell. HRTEM images of obtained catalyst (Fig. 2A and B) confirmed the stability of the core–shell system in Fe_3O_4@SiO_2 nanoparticles after modification. Moreover, FESEM analysis indicated our mentioned catalyst has a spherical uniform morphology and smooth surface (Fig. 2C and D).

We also explored the magnetization of magnetic nanoparticles by vibrating sample magnetometer (VSM) at room temperature (Fig. 3A). The superparamagnetic behavior for our catalyst was confirmed with the field-dependent magnetization curves without any coercivity field (H_c) and remanent magnetism (M_r). The resulted data in Fig. 3A shows the high saturation magnetization (M_s) of about 22 emu g^{-1} for the catalyst that enables it to be easily separated *via* an external magnet from the reaction mixture.[21] According to TGA curve of catalyst initial weight at 0–200 °C can be related to trapped solvent on the surface of the catalyst (Fig. S3B†). As can be seen in Fig. 3B, main weight loss for the catalyst (Fe_3O_4@SiO_2-APTES-MnL^{GDC}) is observed at high temperature of about 300–600 °C which proved thermal stability of the final catalyst. Thermal behaviour of Fe_3O_4@SiO_2-APTES-H_2L^{GDC} and Fe_3O_4@SiO_2-APTES-MnL^{GDC} samples under N_2 atmosphere showed same decomposition pattern indicating that under metalation with Mn the total structure was preserved. A noticeable point in this matter is that after metalation with Mn the temperature range of main weight loss has been shifted to the lower temperatures (compare diagrams c and d in Fig. 3B). This issue can be attributed to the catalytic role of Mn on the decomposition process of organic moieties in the circumstance of TG experiment. Furthermore, the loading of aminopropyl in Fe_3O_4@SiO_2-APTES and ligand in Fe_3O_4@SiO_2-APTES-H_2L^{GDC} achieved about 1.43 and 0.5 mmol g^{-1}, respectively. Further tests such as CHN analysis corroborated these results (1.35 mmol g^{-1} of APTES in Fe_3O_4@SiO_2-APTES and 0.56 mmol g^{-1} of H_3L^{GDC} in Fe_3O_4@SiO_2-APTES-H_2L^{GDC}). In an attempt to do the estimation of manganese loading, we used the AAS technique (was found to be 0.49 mmol g^{-1}).

Chemical state and composition of Mn, Si, C, Cl and O of the mentioned synthesis catalyst were investigated *via* X-ray Photoelectron Spectroscopy (XPS), as well as Fe in the core (Fe_3O_4) (Fig. 4). Achieved data suggest Mn has +3 oxidation state and at 641, and 653 eV we can see lines regarding Mn $2p_{3/2}$ and Mn $2p_{1/2}$, respectively. The presence of iron(III) and (II) in the catalyst was confirmed according to the peaks at 55 (Fe 3p), 710 (Fe $2p_{3/2}$), and 724 eV (Fe $2p_{1/2}$) in Fig. 4D. In addition, appeared peak at 200 eV (Cl 2p) truly proves successful attachment of mentioned ligand (H_3L^{GDC}) on the magnetic nanoparticles (Fig. 4B). As we can see in Fig. 4, peaks related to C 1s, O 1s, Si

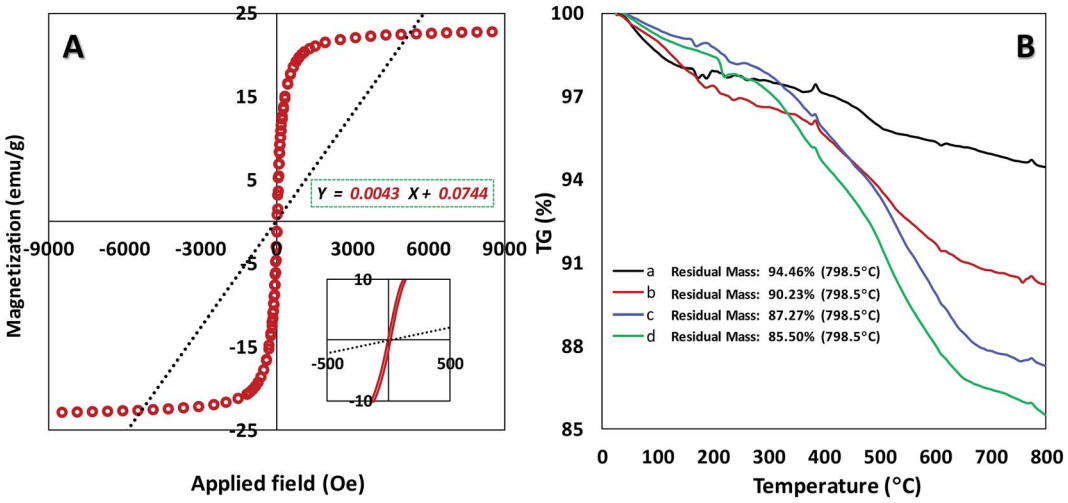

Fig. 3 (A) Magnetization curves of Fe_3O_4@SiO_2-APTES-MnL^{GDC}. Inset: the enlarged image near the coercive field. (B) Thermo-gravimetric analysis (TGA) of Fe_3O_4@SiO_2 (a), Fe_3O_4@SiO_2-APTES (b), Fe_3O_4@SiO_2-APTES-H_2L^{GDC} (c), Fe_3O_4@SiO_2-APTES-MnL^{GDC} (d).

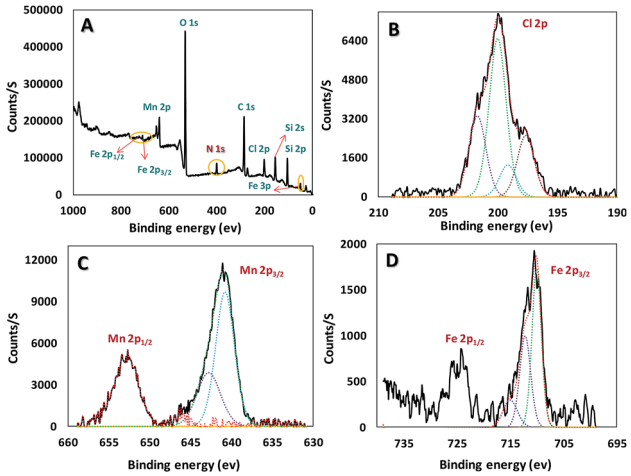

Fig. 4 The X-ray photoelectron spectroscopy (XPS) spectrum of catalyst (Fe_3O_4@SiO_2-APTES-MnL^{GDC}).

2s, Si 2p, and N 1s prove the presence of these elements in our catalyst.[22]

Catalytic activity evaluation

On the basis of the main goal of our studies, we have investigated the efficiency of our designed system for activation of a broad range of substrates with different ability to activation. In an attempt to achieve an optimized condition, we selected oxidation of ethylbenzene to corresponding products as a model reaction (The results are summarized in Table 1, and Fig. S3–S27†). We began our investigation into the effect of solvents such as dioxan, EtOH, THF, and CH_3CN during 5 h; as we can see in Table 1 (entries 1–4) CH_3CN acts as a suitable solvent and the activity of the mentioned catalyst was increased in the smaller amount of CH_3CN (Table 1, entries 4–7). Given the high activity of the catalyst in the absence of solvent, so we evaluated the eligibility of our proposed system in the solvent free condition (Table 1, entry 8). The model reaction in the presence of H_2O_2 cannot progress (Table 1, entry 15); therefore other green oxidants such as O_2 and TBHP were selected.

According to the Table 1 (entries 8–11), our catalyst has the best activity in the presence of 3 eq. TBHP. In order to find the optimized temperature at room temperature, and 70 °C about 13 and 65% conversion was achieved, respectively. Hence, 60 °C was selected as optimized temperature (Table 1 entries 12 and 13). By reducing the amount of catalyst to 1 mol% (20 mg) catalytic activity was decreased (Table 1, entry 14) so 2 mol% catalyst chosen as the optimum amount of catalyst. The experiment was continued by investigation the effect of Fe_3O_4, Fe_3O_4@SiO_2, Fe_3O_4@SiO_2-APTES, and Fe_3O_4@SiO_2-APTES-H_3L^{GDC} (Table 1, entries 16–19). Slightly progress in the model reaction in the presence of them proves that these particles do not have any catalytic activity in this reaction. Moreover, by synthesizing the homogeneous catalyst (MnL^{GDC}), we explored the catalytic activity of this form of catalyst and just about 19% conversion was achieved (Table 1 entry 20). As shown in Fig. S41,† the absorption spectra for the fresh reaction mixture in the presence of MnL^{GDC} after an hour has been changed, this can be duo to the decomposition of homogeneous form of the catalyst (MnL^{GDC}) during the oxidation process. This result clearly confirms the positive effect of nanoparticles on the stability of manganese complex and proves our complex has a good structural stability on the magnetic nanoparticles in the heterogeneous form of our catalyst. It is important to note that, the mentioned reaction in the presence of manganese(II) chloride salt as a catalyst has not a good conversion (Table 1, entry 21). Consequently, the last results strongly proved the dramatically influence of magnetic nanoparticles supported ligand on the activity of catalyst system. It is more notable, in the absence of the catalyst but in the presence of 4 eq. of TBHP, slightly progress in the modal reaction truly confirms the eligibility of our system (Table 1, entries 22 and 23).

In the process of investigation, the high efficiency of mentioned catalyst in the aerobic oxidation of the ethylbenzene in the presence of air and O_2 was checked. In the presence of 2 eq. of TBHP and O_2 our catalyst showed same activity similar to 3 mmol of TBHP without O_2 (Table 1 entries 8 and 10) but at 60 °C and in the absence of TBHP trace conversion was achieved (Table 1, entry 24). Our results show that this oxidant (O_2) can act at a higher temperature and longer time. This point of view is supported by good resulted data in Scheme 2 (Scheme 2b and c, Fig. S29 and 30†). These data confirm the eligibility of our catalyst not only by TBHP (Scheme 2a, Fig. S28†) but also by O_2.

Into confirming the efficiency of the proposed system as an ideal candidate for C–H bond activation, further investigations were continued for a broad range of substrates (Table 2, Fig. S31–S39† and ^{1}H NMR spectrum of products Fig. S42–S49†). 1-Ethyl-4-methoxybenzene (Table 2 entry 1) and 1-ethyl-4-bromobenzene (Table 2, entry 2) were chosen to peruse the effect of electron donating (MeO^-) and electron withdrawing (Br^-) groups in comparison with ethylbenzene. Based on Table 2, the substrate with the electron donating group, converted to products easier than substrates contain electron withdrawing groups. The harder reaction of C–H bond in 1-ethyl-2-bromobenzene (Table 2 entry 3) in comparison with 1-ethyl-4-bromobenzene, causes by the steric effect of bromo group. For bulky molecule such as diphenylmethane, our catalyst showed high activity and selectivity (Table 2 entry 4). It should be noted that high selectivity of the catalyst in a catalytic reaction is as important as high activity. This point of view was confirmed in the oxidation of 1,2,3,4-tetrahydronaphthalene to α-tetralone with high conversion and selectivity in 10 h in the presence of 2 eq. of TBHP (Table 2, entry 5). Furthermore, the designed catalyst showed a good efficiency for oxidation of 1-indanone without any C–C bond cleavage (Table 2 entry 6).

With respect to the industrial application of caprolactam, so direct oxidation of toluene to benzoic acid as one of the important steps for synthesis of caprolactam is so remarkable.[23] Therefore we investigated the competency of our introduced system for direct oxidation of toluene to benzoic acid as interesting transformation. As we can see in Table 2 (entries 7 and 8) our catalyst demonstrated high activity in mentioned reaction and 71% benzoic acid was achieved with 100% selectivity at 20 h. Moreover, to further investigation direct oxidation of 4-methylanisole was performed (Table 2 entry 9) and 83% 4-

Table 1 Optimization for the oxidation of ethylbenzene

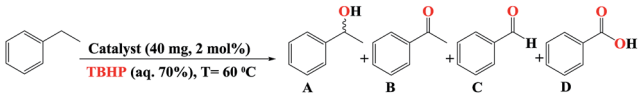

Entry	TBHP (eq.)	Solvent (mL)	Time (h)	Conv.[o] (%)	Selectivity[p] (%) A	B	C	TON[q]
1				16		87	13	16
2	3	THF, 3	5	Trace				
3	3	EtOH, 3	5	Trace				
4	3	CH_3CN, 3	5	39		97	3	39
5	3	CH_3CN, 2	5	41		95	5	41
6	3	CH_3CN, 1	5	47		96	4	47
7	3	CH_3CN, 0.5	5	55		96	4	55
8	3	—[n]	5	62	3	95	2	61
9	2	—	5	49		94	6	49
10[a]	2	—	5	71	2	97	1	70
11	4	—	5	65	2	97	1	65
12[b]	3	—	5	13		92	8	13
13[c]	3	—	5	65		97	3	65
14[d]	3	—	5	50	2	92	6	49
15[e]	—	—	5	Trace				
16[f]	3	—	10	Trace				
17[g]	3	—	10	Trace				
18[h]	3	—	10	Trace				
19[i]	3	—	10	Trace				
20[j]	3	—	10	19		89	11	19
21[k]	3	—	10	30		90	10	30
22[l]	4	—	10	Trace				
23[l]	4	CH_3CN, 0.5	10	Trace				
24[m]	—	CH_3CN, 0.5	10	Trace				
25	2	—	10	70		99	1	70
26	**3**	**—**	**10**	**96**		**98**	**2**	**96**

[a] TBHP (2 eq., 70%), O_2 balloon. [b] T = RT. [c] T = 70 °C. [d] Cat. (20, 1 mol%). [e] H_2O_2 (3 eq., 30%). [f] Fe_3O_4, 40 mg. [g] Fe_3O_4@SiO_2, 40 mg. [h] Fe_3O_4@SiO_2-APTES, 40 mg. [i] Fe_3O_4@SiO_2-APTES-H_2L^{GDC}, 40 mg. [j] MnL^{GDC} (10 mg, 2 mol%). [k] $MnCl_2 \cdot 4H_2O$ (4 mg, 2 mol%). [l] In the absence of catalyst. [m] O_2 balloon, in the absence of TBHP. [n] Solvent free. [o] Conversions were determined by GC (anisole as internal standard (1 mmol, 1/1, substrate/anisole)). [p] Selectivity to product = [product%/(products%)] × 100. [q] TON = (substrate/catalyst) × conversion.

methoxybenzoic acid as the main product was obtained and this percentage of conversion proves the positive effect of electron donating group (MeO^-).

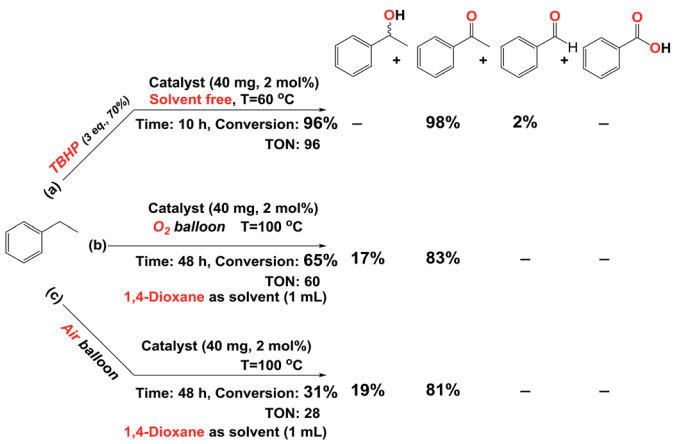

Scheme 2 Oxidation of ethylbenzene catalyzed by catalyst (Fe_3O_4@SiO_2-APTES-MnL^{GDC}) in the presence of (a) TBHP (aq. 70%). (b) O_2. (c) Air.

Monitoring, hot filtration test and recovery of the catalyst

As we can see in Fig. 5A the oxidation reaction of ethylbenzene was monitored as a function of time and 97% of conversion was achieved after 10 h. Moreover, after removal of the catalyst at the half of the completion reaction time (5 h) less than 10% progress in conversion was observed. Also, the amount leaching of manganese into the final aqueous phase was checked and negligible leaching based on the ICP-AES analysis (less than the detection limit) was detected. These results truly confirmed the heterogeneous nature of our catalytic system.

It is noteworthy that simple separation and good recovery of the catalyst is one of the important branches of green chemistry, accordingly, to further validation of our catalytic system the feasibility of catalyst recovery was investigated for oxidation of ethylbenzene under optimal condition (Fig. 5B). Five successive recycling of catalyst is a good validation on the durability of our catalyst. In addition, XRD patterns (Fig. 1A and S1B†), FESEM image (Fig. 2C and D and S1A†), VSM data (Fig. 3A and S2A†) as well as TGA analysis (Fig. 3B and S2B†) of pristine and recovered catalysts clearly show the high chemical and physical stability of our catalysts. The

Table 2 Substrate scope catalyzed by Fe_3O_4@SiO_2-APTES-MnL^{GDC}

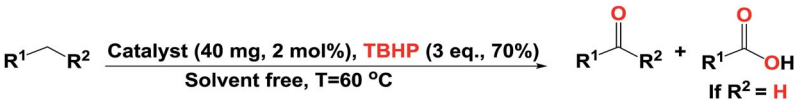

Entry	Substrate	Major product	Time (h)	Conv.[c] (%)	Selectivity[d] (%) Major product	Other product	TON[e]
1	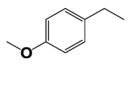	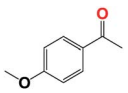			91	9	92
2	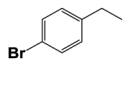	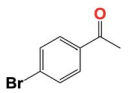	10	96	98	2	95
3			10	64	48	52	47
4	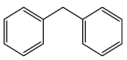	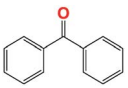	10	93	100	—	93
5[a]			10	91	91	9	89
6		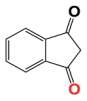	10	80	100	—	80
7[b]		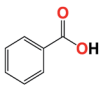	10	57	100	—	86
8[b]		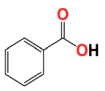	20	71	100	—	107
9[b]	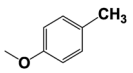	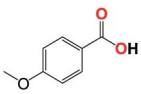	20	87	92	8	131

[a] TBHP (2 eq., 70%). [b] TBHP (4 eq., 70%). [c] Conversions were determined by GC. [d] Selectivity to product = [product%/(products%)] × 100. [e] TON = (substrate/catalyst) × conversion.

Mn content of the recovered catalyst was determined by AAS technique. The result indicated a small leaching in the Mn content at the end of recovery process (0.49 mmol g^{-1} for fresh catalyst *vs.* 0.47 mmol g^{-1} for recovered catalyst). It may be concluded that the negligible decreasing of catalytic activity after the 5th run could be attributed to this minimal leaching of Mn species and/or small losing of catalyst mass during the recovery process.

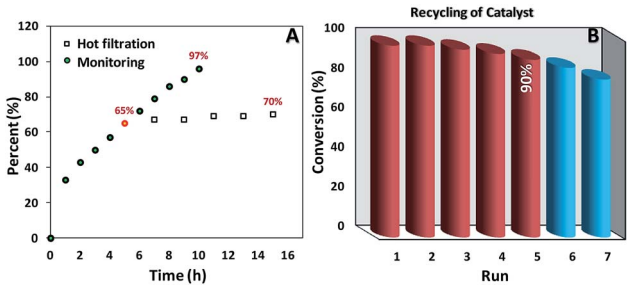

Fig. 5 (A) Monitoring and hot filtration test, (B) recycling for oxidation of ethylbenzene.

Proposed mechanism

According to the previous studies, the oxidation mechanism of C–H bond in the presence of a non-heme manganese complex involves a high-valent manganese-oxo species.

Therefore, we think that our system containing a non-heme manganese complex can produce metal-oxo species which can generate short-lived alkyl radicals in this reaction (Scheme 3, cycle A). As can be seen in following Scheme (cycle B), the formed alcohol converts to the aldehyde or ketone form. Also,

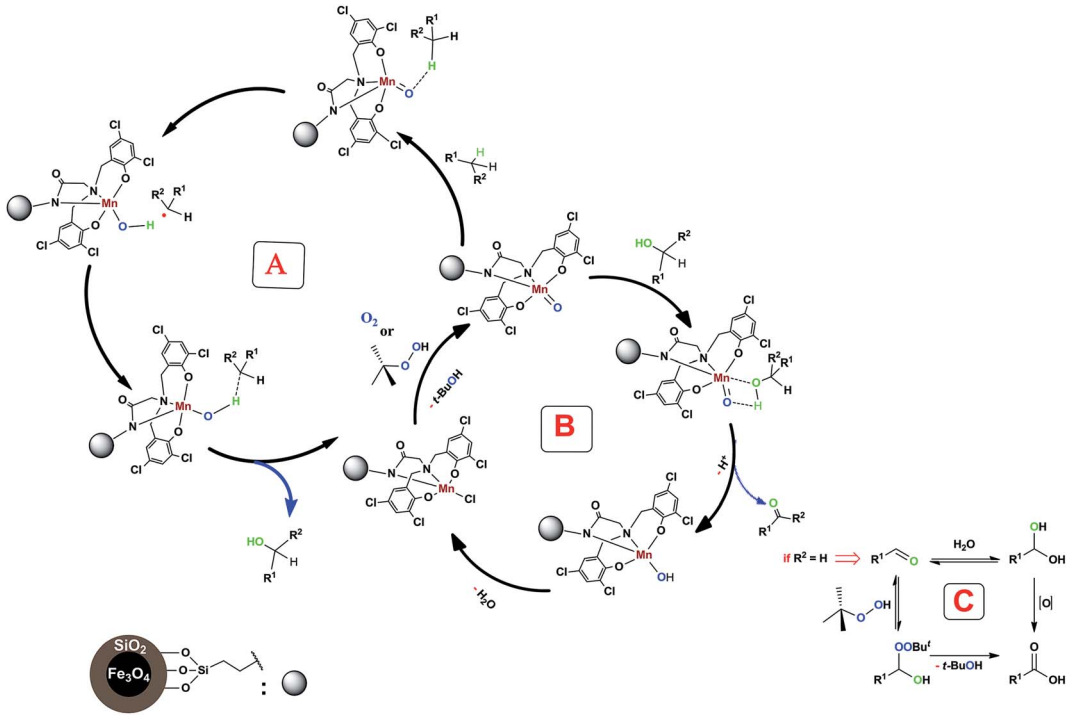

Scheme 3 Proposed mechanism for our non-heme manganese complex-catalyzed benzylic C–H bond oxidation reaction.

further oxidation of prepared benzaldehydes by using of oxidant (TBHP) or H_2O can be done (Scheme 3, cycle C).[24]

Conclusions

In conclusion, our reported system consisting of three parts, Mn(III) ion, amine bis(phenol) ligand (H_3L^{GDC}) and magnetic nanoparticles. These components showed a good cooperation effect acting as an efficient, recyclable and environmentally friendly catalyst under solvent-free and mild conditions in benzylic C–H bond oxidation reaction for a variety of substrates as well as toluene. The chemical nature and structural stability of the catalyst were confirmed by various techniques. Furthermore, both the leaching experiment and five successive recycling of the catalyst, proved the strong attachment of the manganese complex onto the magnetite nanoparticles.

Experimental section

Materials and methods

All reagents and solvents were purchased from commercial sources and used without further purification. Fourier transform infrared spectroscopy on KBr pellets of the compounds was recorded on a Bruker Vector 22 in the range of 400 and 4000 cm^{-1}. UV-vis absorbance digitized spectra were collected using a CARY 100 spectrophotometer. The morphological features of particles were characterized by using field emission transmission electron microscopy (JEOL, JEM-2100F, 200 kV TEM) and Field emission scanning electron microscopy (JEOL, JSM-7610F). Elemental analyses (C, H and N) were performed by the Elementar, Vario EL III. The X-ray powder patterns were recorded using a PHILIPS PW1730 (step size: 0.05, time per step: 1 s). The content of manganese in the catalyst was determined using an Atomic Absorption Spectrometer Varian Spectre AA 110. The organic composition of the modified MNPs base materials was determined by thermogravimetric analysis (TGA) and differential thermoanalysis (DTG), heating from room temperature to 800 °C under nitrogen flow using a STA 409 PC/PG analyser (Netzsch). The magnetic properties of the prepared materials were measured using a homemade vibrating sample magnetometer (Meghnatis Daghigh Kavir Company, Iran) at room temperature from −10 000 to +10 000 Oe. The electronic states of powders were evaluated using X-ray photoelectron spectroscopy (was performed using a Thermo Scientific, ESCALAB 250Xi with Mg X-ray resource). The content of Mn in final aqueous phase was determined by applying an inductively coupled plasma-optical emission spectrometer (ICP-OES). Furthermore, the products were determined and analysed using a VARIAN CP-3800 gas chromatograph equipped with a capillary column and a flame-ionization detector.

Synthesis of Mn(III) complex of Fe_3O_4@SiO_2-APTES-H_2L^{GDC} (Fe_3O_4@SiO_2-APTES-MnL^{GDC})

For synthesis of our catalyst, triethylamine (2 mmol, 0.20 g) was added to a stirred mixture of Fe_3O_4@SiO_2-APTES-H_2L^{GDC} (1.00 g) and $MnCl_2 \cdot 4H_2O$ (1 mmol, 0.20 g) in ethanol (80 mL) under continuous stirring. The mixture reaction was stirred at room temperature for 4 days. Final product was separated from the reaction mixture by applying an external magnetic field and washed with ethanol and acetone. The resulting solid was dried at 80 °C overnight and used for high selective oxidation of benzylic C–H bonds. The resulting material was denoted as Fe_3O_4@SiO_2-APTES-MnL^{GDC}.

General procedure in the C–H bond oxidation

Under atmosphere of argon in a 5 mL glass flask were placed catalyst (0.04 g, 2 mol%) and substrate (1 mmol) in solvent free condition, TBHP as oxidant was added. The reaction mixture was continuously stirred at 60 °C for the desired time and the reaction was monitored by TLC, after completion of the reaction, anisole (1 mmol, 1/1 substrate and anisole) as internal standard was added. In continue the mixture was extracted with ethyl acetate and then the catalyst was magnetically recovered by placing a permanent magnet in the reactor wall. Products were collected with a syringe and analyzed by gas chromatography (GC). The catalyst was washed several times with ethanol and acetone and then dried at 80 °C overnight before being used again for the next reaction.

Conflicts of interest

There are no conflicts to declare.

Acknowledgements

The authors are grateful to the Institute for Advanced Studies in Basic Sciences (IASBS), the chemistry department of Shiraz University and Bahman Farnoudi for proofreading of the manuscript.

Notes and references

1 (*a*) J. Wencel-Delord and F. Glorius, *Nat. Chem.*, 2013, **5**, 369–375; (*b*) K. Godula and D. Sames, *Science*, 2006, **312**, 67–72.
2 (*a*) M. Chen, Y. Pan, H.-K. Kwong, R. J. Zeng, K.-C. Lau and T.-C. Lau, *Chem. Commun.*, 2015, **51**, 13686–13689; (*b*) R. Banerjee, Y. Proshlyakov, J. D. Lipscomb and D. A. Proshlyakov, *Nature*, 2015, **518**, 431–434; (*c*) R. Balasubramanian, S. M. Smith, S. Rawat, L. A. Yatsunyk, T. L. Stemmler and A. C. Rosenzweig, *Nature*, 2010, **465**, 115–119; (*d*) G. Xue, D. Wang, R. De Hont, A. T. Fiedler, X. Shan, E. Münck and L. Que, *Proc. Natl. Acad. Sci. U. S. A.*, 2007, **104**, 20713–20718; (*e*) C. E. Tinberg and S. J. Lippard, *Acc. Chem. Res.*, 2011, **44**, 280–288; (*f*) D. Wang, E. R. Farquhar, A. Stubna, E. Münck and L. Que, *Nat. Chem.*, 2009, **1**, 145–150.
3 V. C. C. Wang, S. Maji, P. P. Y. Chen, H. K. Lee, S. S. F. Yu and S. I. Chan, *Chem. Rev.*, 2017, **117**, 8574–8621.
4 (*a*) J. Rittle and M. T. Green, *Science*, 2010, **330**, 933–937; (*b*) B. Meunier, S. P. de Visser and S. Shaik, *Chem. Rev.*, 2004, **104**, 3947–3980.
5 (*a*) J.-M. Li, Y.-H. Wang, Y. Yu, R.-B. Wu, J. Weng and G. Lu, *ACS Catal.*, 2017, **7**, 2661–2667; (*b*) S. Tang, P. Wang, H. Li and A. Lei, *Nat. Commun.*, 2016, **7**, 11676.
6 (*a*) S. Rana, A. Dey and D. Maiti, *Chem. Commun.*, 2015, **51**, 14469–14472; (*b*) J. Serrano-Plana, W. N. Oloo, L. Acosta-Rueda, K. K. Meier, B. Verdejo, E. García-España, M. G. Basallote, E. Münck, L. Que, A. Company and M. Costas, *J. Am. Chem. Soc.*, 2015, **137**, 15833–15842.
7 (*a*) A. Conde, G. Sabenya, M. Rodríguez, V. Postils, J. M. Luis, M. M. Díaz-Requejo, M. Costas and P. J. Pérez, *Angew. Chem., Int. Ed.*, 2016, **55**, 6530–6534; (*b*) L. Carroll, H. L. Evans, A. C. Spivey and E. O. Aboagye, *Chem. Commun.*, 2015, **51**, 8439–8441.
8 (*a*) H. Ren, Y.-P. Zhou, Y. Bai, C. Cui and M. Driess, *Chem.–Eur. J.*, 2017, **23**, 5663–5667; (*b*) F. Yang, J. Yu, Y. Liu and J. Zhu, *Org. Lett.*, 2017, **19**, 2885–2888.
9 (*a*) Z. Ruan, D. Ghorai, G. Zanoni and L. Ackermann, *Chem. Commun.*, 2017, **53**, 9113–9116; (*b*) Y. He, Y. Cai and S. Zhu, *J. Am. Chem. Soc.*, 2017, **139**, 1061–1064.
10 (*a*) M. D. K. Boele, G. P. F. van Strijdonck, A. H. M. de Vries, P. C. J. Kamer, J. G. de Vries and P. W. N. M. van Leeuwen, *J. Am. Chem. Soc.*, 2002, **124**, 1586–1587; (*b*) R. Shi, H. Niu, L. Lu and A. Lei, *Chem. Commun.*, 2017, **53**, 1908–1911; (*c*) J. L. Nallasivam and R. A. Fernandes, *J. Am. Chem. Soc.*, 2016, **138**, 13238–13245.
11 C.-Q. Wang, L. Ye, C. Feng and T.-P. Loh, *J. Am. Chem. Soc.*, 2017, **139**, 1762–1765.
12 X. Wu, B. Wang, S. Zhou, Y. Zhou and H. Liu, *ACS Catal.*, 2017, **7**, 2494–2499.
13 B. C. Bailey, H. Fan, J. C. Huffman, M.-H. Baik and D. J. Mindiola, *J. Am. Chem. Soc.*, 2007, **129**, 8781–8793.
14 (*a*) A.-H. Lu, E. L. Salabas and F. Schüth, *Angew. Chem., Int. Ed.*, 2007, **46**, 1222–1244; (*b*) S. Shylesh, V. Schünemann and W. R. Thiel, *Angew. Chem., Int. Ed.*, 2010, **49**, 3428–3459.
15 (*a*) S. Vásquez-Céspedes, K. M. Chepiga, N. Möller, A. H. Schäfer and F. Glorius, *ACS Catal.*, 2016, **6**, 5954–5961; (*b*) M. Kaur, S. Pramanik, M. Kumar and V. Bhalla, *ACS Catal.*, 2017, **7**, 2007–2021; (*c*) S. Warratz, D. J. Burns, C. Zhu, K. Korvorapun, T. Rogge, J. Scholz, C. Jooss, D. Gelman and L. Ackermann, *Angew. Chem., Int. Ed.*, 2017, **56**, 1557–1560; (*d*) Y. Gao, P. Tang, H. Zhou, W. Zhang, H. Yang, N. Yan, G. Hu, D. Mei, J. Wang and D. Ma, *Angew. Chem., Int. Ed.*, 2016, **55**, 3124–3128; (*e*) T. V. Tran, H. T. N. Le, H. Q. Ha, X. N. T. Duong, L. H. T. Nguyen, T. L. H. Doan, H. L. Nguyen and T. Truong, *Catal. Sci. Technol.*, 2017, **7**, 3453–3458; (*f*) X. Tian, F. Yang, D. Rasina, M. Bauer, S. Warratz, F. Ferlin, L. Vaccaro and L. Ackermann, *Chem. Commun.*, 2016, **52**, 9777–9780; (*g*) S. Korwar, M. Burkholder, S. E. Gilliland, K. Brinkley, B. F. Gupton and K. C. Ellis, *Chem. Commun.*, 2017, **53**, 7022–7025; (*h*) B. Dong, Z. Han, Y. Zhang, Y. Yu, A. Kong and Y. Shan, *Chem.–Eur. J.*, 2016, **22**, 2046–2050; (*i*) V. Pascanu, F. Carson, M. V. Solano, J. Su, X. Zou, M. J. Johansson and B. Martín-Matute, *Chem.–Eur. J.*, 2016, **22**, 3729–3737; (*j*) S. Zhang, H. Wang, M. Li, J. Han, X. Liu and J. Gong, *Chem. Sci.*, 2017, **8**, 4489–4496; (*k*) X. Wang, M. Liu, Y. Wang, H. Fan, J. Wu, C. Huang and H. Hou, *Inorg. Chem.*, 2017, **56**, 13329–13336; (*l*) D.-T. D. Tang, K. D. Collins and F. Glorius, *J. Am. Chem. Soc.*, 2013, **135**, 7450–7453; (*m*) H. Fei and S. M. Cohen, *J. Am. Chem. Soc.*, 2015, **137**, 2191–2194.
16 (*a*) C. Rajendran and G. Satishkumar, *ChemCatChem*, 2017, **9**, 1284–1291; (*b*) S. Samanta and R. Srivastava, *Appl. Catal., B*, 2017, **218**, 621–636.

17 (*a*) Y. Kuwahara, Y. Yoshimura and H. Yamashita, *Catal. Sci. Technol.*, 2016, **6**, 442–448; (*b*) S. Singha and K. M. Parida, *Catal. Sci. Technol.*, 2011, **1**, 1496–1505; (*c*) L. Fu, S. Zhao, Y. Chen and Z. Liu, *Chem. Commun.*, 2016, **52**, 5577–5580; (*d*) Y. Aratani, Y. Yamada and S. Fukuzumi, *Chem. Commun.*, 2015, **51**, 4662–4665; (*e*) L. Wang, G. Wang, J. Zhang, C. Bian, X. Meng and F.-S. Xiao, *Nat. Commun.*, 2017, **8**, 15240; (*f*) Y. Li, C. Liu and W. Yang, *New J. Chem.*, 2017, **41**, 8214–8221.

18 T. Karimpour, E. Safaei, B. Karimi and Y. Lee, *ChemCatchem*, 2018, **10**, 1889–1899.

19 (*a*) S. Sun, H. Zeng, D. B. Robinson, S. Raoux, P. M. Rice, S. X. Wang and G. Li, *J. Am. Chem. Soc.*, 2004, **126**, 273–279; (*b*) M. Shao, F. Ning, J. Zhao, M. Wei, D. G. Evans and X. Duan, *J. Am. Chem. Soc.*, 2012, **134**, 1071–1077.

20 Y. Liu, W. Zhang, X. Li, X. Le and J. Ma, *New J. Chem.*, 2015, **39**, 6474–6481.

21 (*a*) X. Dong, X. Zhang, P. Wu, Y. Zhang, B. Liu, H. Hu and G. Xue, *ChemCatChem*, 2016, **8**, 3680–3687; (*b*) R. K. Sharma, M. Yadav, Y. Monga, R. Gaur, A. Adholeya, R. Zboril, R. S. Varma and M. B. Gawande, *ACS Sustainable Chem. Eng.*, 2016, **4**, 1123–1130.

22 (*a*) Y. Liu, J.-F. Chen, J. Bao and Y. Zhang, *ACS Catal.*, 2015, **5**, 3905–3909; (*b*) L. Wang, X. Wang, J. Luo, B. N. Wanjala, C. Wang, N. A. Chernova, M. H. Engelhard, Y. Liu, I.-T. Bae and C.-J. Zhong, *J. Am. Chem. Soc.*, 2010, **132**, 17686–17689.

23 X. Xu, M. Tang, M. Li, H. Li and Y. Wang, *ACS Catal.*, 2014, **4**, 3132–3135.

24 (*a*) M. Guo, T. Corona, K. Ray and W. Nam, *ACS Cent. Sci.*, 2019, **5**, 13–28; (*b*) X. Wu, M. S. Seo, K. M. Davis, Y.-M. Lee, J. Chen, K.-B. Cho, Y. N. Pushkar and W. Nam, *J. Am. Chem. Soc.*, 2011, **133**, 20088–20091; (*c*) A. Gunay and K. H. Theopold, *Chem. Rev.*, 2010, **110**, 1060–1081; (*d*) R. Noyori, M. Aoki and K. Sato, *Chem. Commun.*, 2003, 1977–1986.